Generalized Two-Dimensional Correlation Analysis of NMR and Raman Spectra for Structural Evolution Characterizations of Silk Fibroin

Bing-Wen Hu,[†] Ping Zhou,*[,†] Isao Noda,[‡] and Qing-Xia Ruan[†]

The Key Laboratory of Molecular Engineering of Polymers, Ministry of Education, Department of Macromolecular Science, Fudan University, Shanghai 200433, P. R. China, and The Procter & Gamble Company, 8611 Beckett Road, West Chester, Ohio 45069

Received: April 21, 2006; In Final Form: July 17, 2006

Generalized two-dimensional (2D) correlation spectroscopy was used to characterize the structural evolution of silk fibroin as the pH changed from 6.8 to 4.8, demonstrating that the conformational transitions of silk fibroin are induced step by step as the pH decreases. 2D homo- and hetero-spectral correlation spectroscopy was used to establish the relationship between information extracted from NMR and Raman spectroscopy. This novel method reveals the structural evolution using two probes with different frequency scales (10^{5-9} Hz for nuclear spin motion and 10^{12-14} Hz for molecular vibration motion), reflecting the different spatial scale sensitivity to the molecular conformational change. The transition order is identified as silk I state (helix dominant) → silk I intermediate state → silk II intermediate state → silk II state (β-sheet dominant), as the pH decreases. The results may rationalize the silkworm spinning process, which undergoes the conformational transition steadily from the soluble helix state to the insoluble β-sheet state as the pH decreases from the posterior to anterior glands.

Silk fiber from *Bombyx mori* has been widely investigated because of its mechanical properties, spinning mechanisms, and molecular structures. It has been investigated using various methods, including rheological,[1−6] spectroscopical,[7−20] and biological methods.[21−26] Many attempts were made to chemically[27−33] and genetically[22,25,26,34] synthesize fibers such as silk fibers, but these failed to succeed in producing satisfactory fibers with comparable properties. There are still many basic issues on fibroin structure and spinning dynamics, which play important roles but are not yet fully understood by scientists. The natural fibroin spinning process involves many conditional changes, such as changes in pH,[1,5,35,36] in fibroin concentration,[1] in shearing force,[1−5,36] and in metal ions,[19,35] which, in turn, result in the fibroin structural changes occurring gradually from the soluble helix conformation to the insoluble β-sheet conformation. These β-sheets are well-oriented along the axis of the fiber, giving it the strength and stiffness comparable or even superior to those of high-performance synthetic materials.

The generalized 2D correlation technique has gained popularity, especially in the optical spectroscopy field (e.g., infrared, Raman, near-infrared, and ultraviolet spectroscopy).[37−42] Recently, it was also used to analyze the NMR diffusion experiment data[43] and the multiple-pulse two-dimensional NMR data.[44] However, surprisingly little has been reported on the application of generalized 2D correlation spectroscopy to the perturbation-based NMR data. In this work, we used a perturbation-based generalized two-dimensional homo- and hetero-spectral correlation spectroscopy to establish the relationship between information extracted from perturbation-based 1D NMR and Raman spectroscopy. The structural evolution of silk fibroin during the pH change is further investigated on the basis of this novel method with different frequency scales (10^{5-9} Hz for nuclear spin motion and 10^{12-14} Hz for molecular vibration motion), reflecting the different spatial scale sensitivities to conformational changes of molecules.

* To whom correspondence should be addressed. E-mail: pingzhou@fudan.edu.cn. Tel: +86-21-55664038. Fax: +86-21-65640293.

[†] Fudan University.

[‡] The Procter & Gamble Company.

Theoretical Background

Generalized 2D correlation spectroscopy is based on the perturbation of samples with temperature, concentration, reaction time, and so on.

The perturbation-induced changes in spectral intensities $y(\nu,t)$ can be obtained as a function of an exterior perturbation variable t, where the data are collected as t changes from $T_{\min}$ to $T_{\max}$. Here, t can be any reasonable physical variable, such as the change in the pH value, as used in the present work. The perturbation-based spectral profile $\tilde{y}(\nu,t)$ is expressed as

$$\tilde{y}(\nu,t) = \begin{cases} y(\nu,t) - \bar{y}(\nu) & \text{for } T_{\min} \le t \le T_{\max} \\ 0 & \text{otherwise} \end{cases} \quad (1)$$

where $\bar{y}(\nu)$ is an average of the trace profiles obtained over the observed perturbation range and is used as a reference spectrum:

$$\bar{y}(\nu) = \frac{1}{T_{\max} - T_{\min}} \int_{T_{\min}}^{T_{\max}} y(\nu,t)\, dt \quad (2)$$

The generalized 2D correlation function for the perturbation-based spectra is defined as[37,42]

$$\Phi(\nu_1,\nu_2) + i\Psi(\nu_1,\nu_2) = \frac{1}{\pi(T_{\max} - T_{\min})} \int_0^\infty \tilde{z}_1(\nu_1,\omega) \times \tilde{z}_2^*(\nu_2,\omega)\, d\omega \quad (3)$$

where $\Phi(\nu_1,\nu_2)$ and $\Psi(\nu_1,\nu_2)$ are called respectively generalized synchronous and asynchronous 2D correlation spectra. $\tilde{z}_1(\nu_1,\omega)$

10.1021/jp062461y CCC: $33.50
Published on Web 08/22/2006

is the Fourier transformation of the data $\tilde{y}_1(\nu_1,t)$, and $\tilde{z}_2^*(\nu_2,\omega)$ is the corresponding Fourier conjugate of the data $\tilde{y}_2(\nu_2,t)$.

When $\tilde{y}_1(\nu_1,t)$ and $\tilde{y}_2(\nu_2,t)$ are recorded by the same spectroscopic technique, for example, by NMR spectroscopy, the two-dimensional correlation technique is called generalized 2D homo-spectral correlation spectroscopy. In contrast, if $\tilde{y}_1(\nu_1,t)$ and $\tilde{y}_2(\nu_2,t)$ are recorded with different probes, such as with Raman and NMR spectroscopy under the same perturbation, it is called generalized 2D hetero-spectral correlation spectroscopy.

A cross-peak (ν_1,ν_2) found in a synchronous 2D correlation spectrum $\Phi(\nu_1,\nu_2)$ represents the simultaneous or coincidental changes in spectral intensities observed by spectroscopic techniques 1 and 2 at corresponding variables ν_1 and ν_2, as an external perturbation is applied. Here, techniques 1 and 2 can be based on the same spectroscopic probe or on two different ones (so-called hetero-spectral correlation). The sign of a synchronous cross-peak becomes positive if the response at ν_1 is in the same direction as that at ν_2, either increasing or decreasing simultaneously, as the external physical variable (e.g., pH) is changed. In contrast, a negative cross-peak indicates that the response at ν_1 is in the opposite direction to that at ν_2 .

A cross-peak present in an asynchronous 2D correlation spectrum $\Psi(\nu_1,\nu_2)$ indicates that the responses observed by spectroscopic techniques one and two at corresponding variables ν_1 and ν_2 vary out of phase with each other as the perturbation is applied. The response at ν_1 occurs earlier than that at ν_2 if the signs of the cross-peaks (ν_1, ν_2) in both synchronous and asynchronous spectra are the same; in contrast, the response at ν_1 occurs later than that at ν_2 if the signs are different.

Experimental Section

Materials. *Bombyx mori* cocoons were degummed in a boiling aqueous Na_2CO_3 (0.5 wt %) solution for 0.5 h. After the degummed silk fibers were thoroughly rinsed with deionized water, the regenerated silk fibroin solution was prepared by dissolving 10 g of the degummed silk fiber in 100 mL of 9.3 M LiBr solution for 1 h at room temperature. The resulting solution was dialyzed against deionized water at ambient temperature for 3 days to remove LiBr. The deionized water was refreshed every 4 h during dialysis. This procedure yielded a 4 wt % silk fibroin stock solution, which was then used to prepare 1 wt % regenerated fibroin solutions at a pH of 6.8, 6.3, 5.8, 5.3, and 4.8 by mixing equivalent volumes of a 2 wt % fibroin solution and a $NaH_2PO_4-Na_2HPO_4$ buffer with the defined pH values.

All the prepared solutions were left to dry at room temperature to form membranes on polyester film surfaces for about 3 days, partially imitating the process of water removal during natural spinning by the silkworm.

Raman Spectroscopy. Raman spectra were recorded using a Dilor LabRam-1B spectrometer, operating at a resolution of 1 cm^{-1}. The Spectra Physics model 164 argon ion laser was operated at 632.8 nm with about 6 mW of power.

^{13}C CP-MAS NMR. ^{13}C cross-polarization magic-angle spinning (CP-MAS) NMR experiments were carried out on a Varian Infinityplus-300 NMR spectrometer operated at 75.3 MHz for ^{13}C resonance with a cross polarization contact time of 1 ms, a pulse repeat time of 3 s, an accumulation of 2000 scans, a ^{1}H 90° pulse width of 4.0 μs, and a high-power ^{1}H-decoupling of 62.5 kHz during signal acquisition. The sample was spun at a rate of 5 kHz in a 7.5 mm spin rotor. Chemical shifts were reported relative to the external reference of adamantine (38.5 ppm).

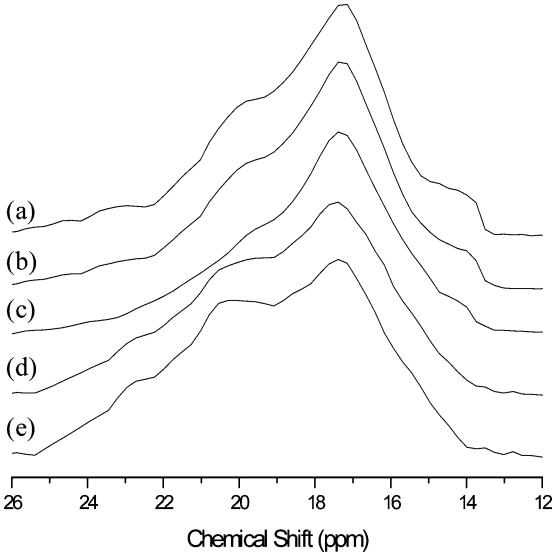

Figure 1. 1D ^{13}C CP-MAS NMR spectra of a series of silk fibroin membranes prepared from regenerated fibroin solutions buffered at pH 6.8 (a), 6.3 (b), 5.8 (c), 5.3 (d), and 4.8 (e).

Generalized 2D Homo- and Hetero-Spectral Correlation Spectra. The 2D correlation spectra were generated by using the POCHA software composed by Daisuke Adachi (Department of Chemistry, Kwansei Gakuin University). The 1D spectra, shown at the side and top of the 2D correlation maps, are the averages of the trace profiles over the pH range and are used as the references.

Results and Discussion

2D NMR−NMR Homo-Spectral Correlation. Perturbation-induced changes in the NMR spectrum $y_1(\nu_1,t)$ are shown in Figure 1. The region of 13−24 ppm in Figure 1 represents the resonance of C_β in alanine residues of silk fibroin and is often used to investigate the conformation of silk fibroin.[20] It is obvious that the NMR spectra change when the pH varies from 6.8 to 4.8.

To reveal more specific information about the silk fibroin conformational transition along with the pH change, the generalized 2D NMR−NMR homo-spectral correlation spectrum is constructed in Figure 2. Five traces are enough to capture all of the pertinent features for the conformation determination. The synchronous 2D correlation spectrum in Figure 2A shows that there are at least two positive cross-peaks (ppm, ppm) around (22.5, 20.5) and (17.5, 14.0), indicating that there are four conformations around 22.5, 20.5, 17.5, and 14.0 ppm, which are also present in Figure 1. It indicates that the conformational response corresponding to 22.5 ppm is similar to that around 20.5 ppm and that the conformational response corresponding to 17.5 ppm is similar to that around 14.0 ppm as the pH decreases from 6.8 to 4.8. The density functional theory (DFT) calculation[45] indicated that the chemical shift of C_β at 20.5 ± 0.5 represents a typical silk II structure and around 22.5 ppm, a silk II-related intermediate; the chemical shift at 17.5 ± 0.5 ppm represents a typical silk I structure and around 14.5 ppm, a silk I-related intermediate. Moreover, four negative cross-peaks (ppm, ppm), (22.5, 17.5), (22.5, 14.0), (20.5, 17.5), and (20.5, 14.0), indicate that the conformations corresponding to 22.5 and 20.5 ppm are different from those corresponding to 17.5 and 14.0 ppm. Furthermore, the signs of cross-peaks (ppm, ppm) (22.5, 20.5) and (17.5, 14.0) in both synchronous and asynchronous spectra are all positive, indicating that the response

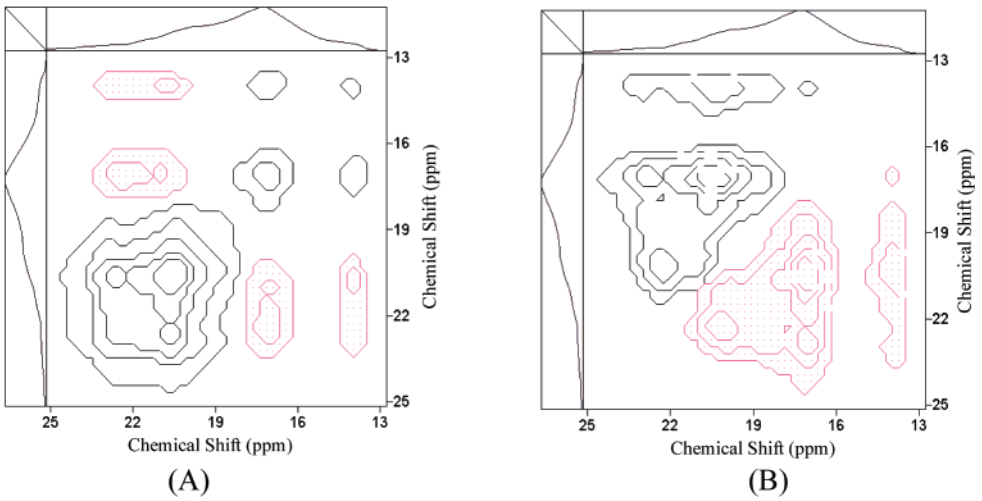

Figure 2. Synchronous (A) and asynchronous (B) 2D NMR−NMR correlation spectra of silk fibroin as the pH decreased from 6.8 to 4.8. Unshaded regions indicate positive correlation intensities; shaded regions indicate negative correlation intensities.

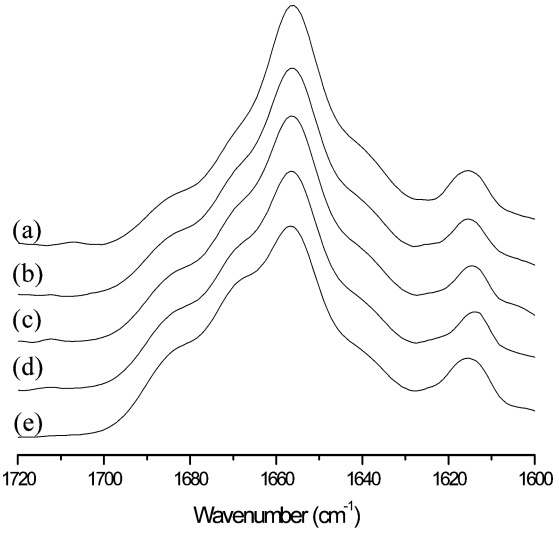

Figure 3. 1D Raman spectra of a series of silk fibroin membranes prepared from regenerated fibroin solutions buffered at pH 6.8 (a), 6.3 (b), 5.8 (c), 5.3 (d), and 4.8 (e).

at 22.5 ppm occurs earlier than that at 20.5 ppm as the pH decreases and that the response at 17.5 ppm occurs earlier than that at 14.0 as the pH decreases. Moreover, the signs of cross-peak (22.5, 14.0) in synchronous and asynchronous spectra are negative and positive, respectively, indicating that the response at 22.5 ppm occurs later than that at 14.0 ppm as the pH decreases. The results reveal that there is a conformational change order, as the pH decreases: 17.5 → 14.0 → 22.5 → 20.5 ppm. The signs from other cross-peaks shown in Figure 2B also confirm this order.

2D Raman−Raman Homo-Spectral Correlation. Perturbation-induced changes in the Raman spectrum $y_2(\nu_2,t)$ are shown in Figure 3; the pH variation is the same as that in the NMR measurement. The peak around 1616 cm^{-1} in Figure 3 is attributed to the aromatic residues of phenylalanine, tyrosine, and tryptophan,[46,47] and the region of 1630−1700 cm^{-1} represents the amide I (C═O stretching) mode of amino acid residues of silk fibroin.

The generalized 2D Raman−Raman homo-spectral correlation spectrum is constructed in Figure 4 with the region 1630−1700 cm^{-1}. The synchronous 2D correlation spectrum (Figure 4A) shows that there are obviously three peaks around 1683, 1668, and 1655 cm^{-1}. The peak around 1642 cm^{-1}, which is not well-resolved in the synchronous 2D correlation spectrum (Figure 4A), can be identified from the asynchronous 2D correlation spectrum (Figure 4B). Thus, there are four conformations corresponding to the peaks around 1683, 1668, 1655, and 1642 cm^{-1} in the Raman spectrum. In the previous work of Monti,[46,47] the peak around 1668 cm^{-1} was assigned to a β-sheet conformation and the peak around 1655 cm^{-1} to a helix conformation, but the conformations of the other two peaks are still unclear. The cross-peaks (cm^{-1}, cm^{-1}) (1683, 1668) and (1683, 1642), which are not well-resolved in the asynchronous 2D Raman−Raman correlation spectrum (Figure 4B), can be identified (see Figure 5) by selecting a slice along 1683 cm^{-1} in Figure 4B. Furthermore, the signs of cross-peaks (cm^{-1}, cm^{-1}) (1655, 1642)[48] and (1683, 1668) in synchronous and asynchronous spectra are all positive, indicating that the response at 1683 cm^{-1} occurs earlier than that at 1668 cm^{-1} and the response at 1655 cm^{-1} occurs earlier than that at 1642 cm^{-1} as the pH decreases. Moreover, the signs of cross-peak (cm^{-1}, cm^{-1}) (1683, 1642) in synchronous and asynchronous spectra are negative and positive, respectively, indicating that the response at 1683 cm^{-1} occurs later than that at 1642 cm^{-1} as the pH decreases . The results reveal that there is a conformational change order as the pH decreases: 1655 → 1642 → 1683 → 1668 cm^{-1}.

2D NMR−Raman Hetero-Spectral Correlation. To establish the relationship of information extracted individually from NMR and Raman spectroscopy, a set of generalized 2D NMR−Raman hetero-spectral correlation spectra are constructed, as shown in Figure 6, using eq 3, on the basis of the data from the NMR spectra in Figure 1 as well as from the Raman spectra in Figure 3.

It is seen from the synchronous 2D correlation spectrum in Figure 6A that the cross-peaks (20.5 ppm, 1668 cm^{-1}), (20.5 ppm, 1683 cm^{-1}), (22.5 ppm, 1668 cm^{-1}) and (22.5 ppm, 1683 cm^{-1}) are all positive, indicating the conformational responses corresponding to the 20.5 and 22.5 ppm peaks in NMR are similar to that corresponding to the 1668 and 1683 cm^{-1} peaks in Raman as the pH decreases. As discussed previously, the 20.5 and 22.5 ppm peaks in NMR represent the silk II and silk II-like states, respectively; the 1668 cm^{-1} peak in Raman represents the silk II state. Therefore, on the basis of the synchronous 2D NMR−Raman correlation spectrum, the 1683 cm^{-1} Raman peak could be assigned to the silk II-like state. In contrast, the cross-peaks (17.5 ppm, 1655 cm^{-1}), (17.5 ppm, 1642 cm^{-1}), (14.0 ppm, 1655 cm^{-1}), and (14.0 ppm, 1642 cm^{-1})

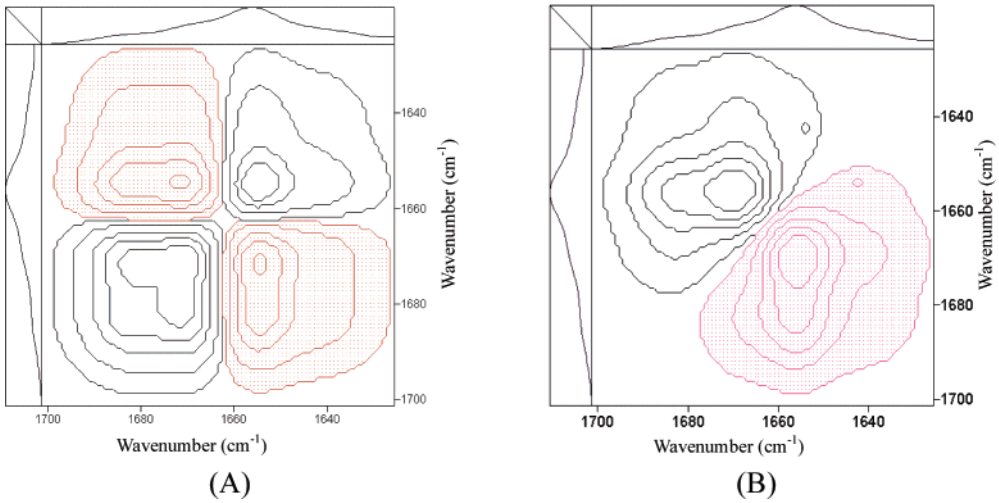

Figure 4. Synchronous (A) and asynchronous (B) 2D Raman−Raman correlation spectra of silk fibroin as the pH decreased from 6.8 to 4.8. Unshaded regions indicate positive correlation intensities; shaded regions indicate negative correlation intensities.

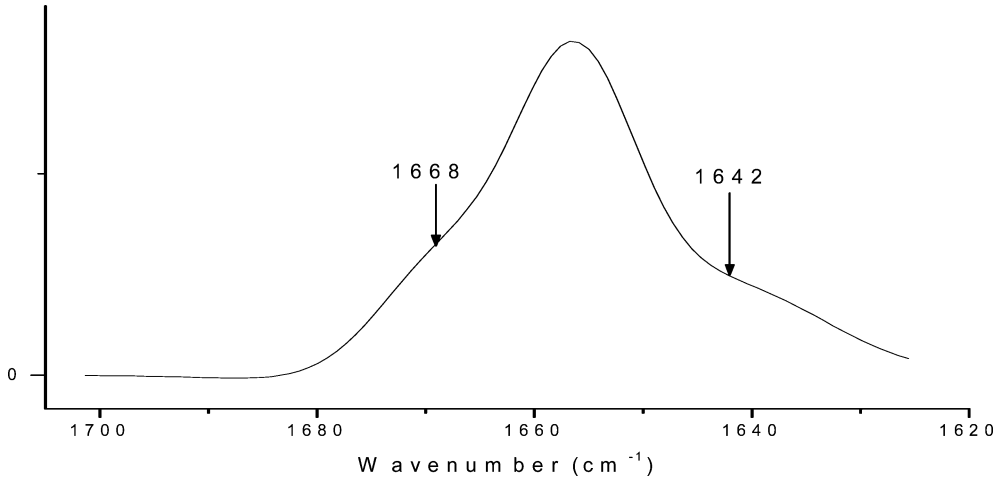

Figure 5. Slice along the 1683 cm^{-1} peak in the asynchronous 2D Raman−Raman correlation spectrum of Figure 4B.

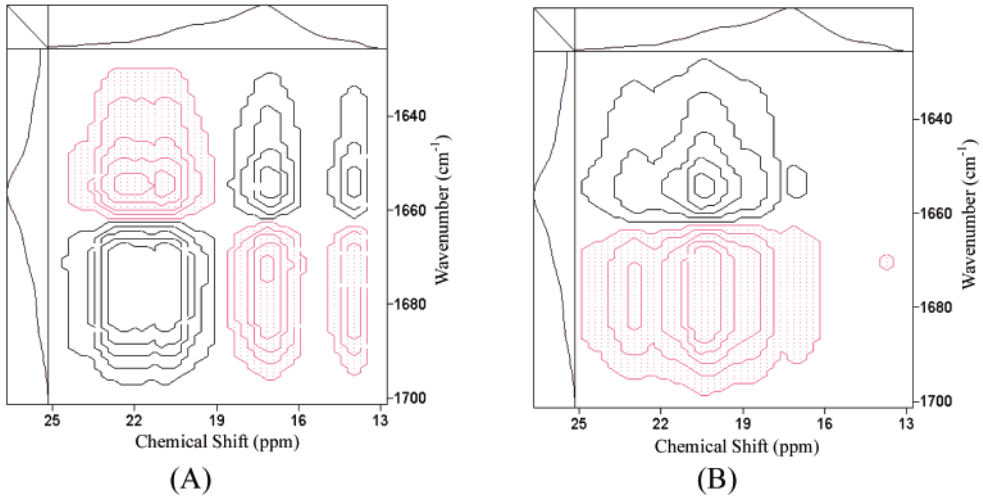

Figure 6. Synchronous (A) and asynchronous (B) 2D NMR−Raman correlation spectra of silk fibroin as the pH decreased from 6.8 to 4.8. Unshaded regions indicate positive correlation intensities; shaded regions indicate negative correlation intensities. The *x* axis is contributed from the NMR spectrum, and the *y* axis is from the Raman spectrum.

are all positive, indicating the conformational responses corresponding to the 17.5 and 14.0 ppm peaks in NMR are similar to that corresponding to the 1655 and 1642 cm^{-1} peaks in Raman. The not well-resolved cross-peaks (17.5 ppm, 1642 cm^{-1}) and (14.0 ppm, 1642 cm^{-1}) can also be identified (see Figure 7) by selecting a slice along the 1642 cm^{-1} peak in Figure 6A. Similarly, it is known that the 17.5 and 14.0 ppm peaks in NMR represent the silk I and silk I-like states, respectively. The 1655 cm^{-1} peak in Raman represents the silk I state; therefore, the 1642 cm^{-1} Raman peak could be assigned to the silk I-like state. Thus, it is deduced on the basis of the result from 2D NMR−NMR and Raman−Raman homo-spectral

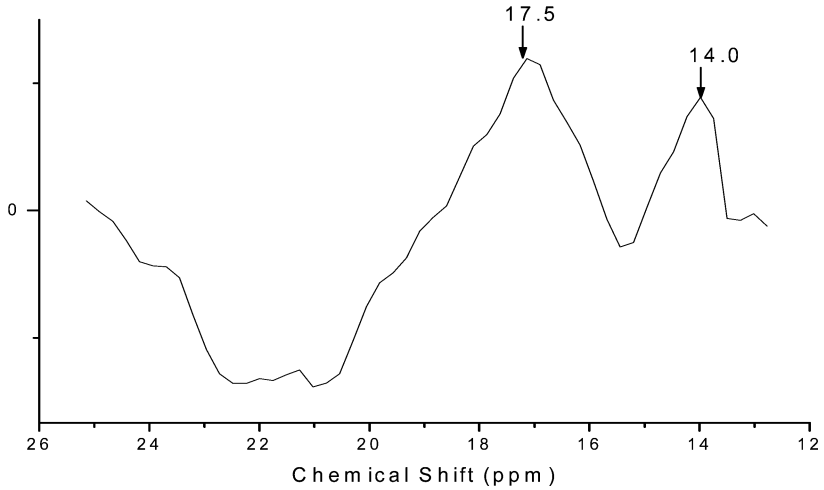

Figure 7. Slice along the 1642 cm^{-1} peak in the synchronous 2D NMR−Raman correlation spectrum of Figure 6A.

correlation spectroscopy together with 2D NMR−Raman heterospectral correlation spectroscopy that, as the pH decreases, there is a transition order: silk I state (17.5 ppm or 1655 cm^{-1}) → silk I-like state (14.0 ppm or 1642 cm^{-1}) → silk II-like state (22.5 ppm or 1683 cm^{-1}) → silk II state (20.5 ppm or 1668 cm^{-1}). Significantly, the fact that the structural relationship is first established by generalized 2D hetero-spectral correlation spectroscopy demonstrates that its application into an unknown molecular structure assignment is reasonable.

In addition, the asynchronous 2D NMR−Raman heterospectral correlation spectrum is shown in Figure 6B. The signs of the region spanning from 22.5 to 18.5 ppm in NMR and from 1665 to 1690 cm^{-1} in Raman (corresponding to silk II-related conformations) in synchronous and asynchronous spectra are positive and negative, respectively, indicating that the response from nuclear spin motion (NMR) in the silk II-related conformation occurs at a later stage than that from molecular vibration (Raman), as the pH is decreased. In contrast, the signs of the region spanning from 17.5 to 16.5 ppm in NMR and from 1660 to 1650 cm^{-1} in Raman (corresponding to silk I-related conformations) in both synchronous and asynchronous spectra are all positive, indicating the response from nuclear spin motion in the silk I-related conformation occurs before that from molecular vibration as the pH decreased because of the silk I-related structure being more irregular than the silk II-related one. This phenomenon may result from the fact that the responses to a specific probe, and therefore, to the scale and nature of molecular level susceptibility, are somewhat different for Raman and NMR. In other words, Raman spectroscopy is probably more sensitive to small changes occurring at a very long distance (i.e., atoms separated by many bonds) as the protein is undergoing the conformational transition, because the cooperative vibration mode involves many atoms within the molecule. Even a small change in conformation has a very profound effect on the molecular vibrations. Generalized 2D hetero-spectral correlation spectroscopy is thus useful in the identification of structures with somewhat different levels of changes in conformations.

Mechanism of the pH-Induced Refolding. Here, generalized 2D homo- and hetero-spectral correlation spectra for NMR and Raman demonstrate that, when the pH decreases from 6.8 to 4.8, which is the pH range from the posterior part to the anterior part of the silkworm gland lumen, the conformation of silk fibroin passes through several intermediate states instead of directly transitioning from helix to β-sheet. Such a process could rationalize a mechanism (so-called nucleation-dependent aggregation) present in silk fibroin that was demonstrated by our previous work.[49] The mechanism means that the conformational transition of silk fibroin, that of changing from the water soluble helix state to the insoluble β-sheet state, involves two steps. The first step is the nucleation. It is a rate-limiting and time-consuming step involving the conversion of the soluble helix state to the insoluble β-sheet nucleus, which is thermodynamically unfavorable. The second step is the aggregation growth. Once the β-sheet nucleus forms, further growth of the β-sheet becomes thermodynamically favorable, resulting in a rapid extension of β-sheet aggregation. As previously discussed, each intermediate state formation from helix to β-sheet may require some time, resulting in the formation of β-sheet nuclei only after a long time. Therefore, this process becomes a time-limiting step for silk fibroin. The nucleation-dependent mechanism concerning the secondary structural transformation of silk fibroin observed in vitro may be postulated to occur in vivo.

Conclusion

In the present work, generalized 2D homo- and hetero-spectral correlation spectroscopy is used to construct the 2D NMR−NMR and Raman−Raman correlation spectra, as well as a 2D NMR−Raman correlation spectrum for the characterization of the silk fibroin structural evolution, as the pH decreased from 6.8 to 4.8. It is revealed that the conformational transitions of silk fibroin are induced step by step as the pH decreases. There exists a transition order: silk I state (helix dominant) → silk I intermediate state → silk II intermediate state → silk II state (β-sheet dominant). The results may rationalize the silkworm spinning process, which undergoes the conformational transition steadily from the soluble helix state to the insoluble β-sheet state as the pH decreases from the posterior gland to the anterior gland. The generalized 2D correlation analysis approach makes the results more informational and convincing and thus, is applicable for other spectroscopy, including the correlation spectroscopy of NMR−IR, NMR−UV, etc.

Acknowledgment. This work was supported by the Natural Science Foundation of China (No. 20274009, 10475017, and 20434010).

References and Notes

(1) Magoshi, J.; Magoshi, Y.; Becker, M. A.; Nakamura, S. In *Polymer Materials Encyclopedia*; Salamone, J. C., Ed.; CRC Press: New York, 1996; Vol. 1, pp 667−679.

(2) Parthasarathy, K. M.; Naresh, M. D.; Arumugam, V.; Subramaniam, V.; Sanjeevi, R. *J. Appl. Polym. Sci.* **1996**, *59*, 2049−2053.
(3) Ochi, A.; Hossain, K. S.; Magoshi, J.; Nemoto, N. *Biomacromolecules* **2002**, *3*, 1187−1196.
(4) Hossain, K. S.; Ohyama, E.; Ochi, A.; Magoshi, J.; Nemoto, N. *J. Phys. Chem. B* **2003**, *107*, 8066−8073.
(5) Terry, A. E.; Knight, D. P.; Porter, D.; Vollrath, F. *Biomacromolecules* **2004**, *5*, 768−772.
(6) Mukhamedzhanova, M. Y.; Takhtaganova, D. B.; Pak, T. S. *Chem. Nat. Compd.* **2001**, *37*, 377−380.
(7) Marsh, R. E.; Corey, R. B.; Pauling, L. *Biochim. Biophys. Acta* **1955**, *16*, 1−34.
(8) Asakura, T.; Watanabe, Y.; Uchida, A.; Minagawa, H. *Macromolecules* **1984**, *17*, 1075−1081.
(9) Canetti, M.; Seves, A.; Secundo, F.; Vecchio, G. *Biopolymers* **1989**, *28*, 1613−1624.
(10) Viney, C.; Huber, A. E.; Dunaway, D. L.; Kerkam, K.; Case, S. T. In *Silk Polymers*; Kaplan, D., Adams, W. W., Farmer, B., Viney, C., Eds.; American Chemical Society: Washington, DC, 1994; Vol. 544, pp 120−136.
(11) Willcox, P. J.; Gido, S. P.; Muller, W.; Kaplan, D. L. *Macromolecules* **1996**, *29*, 5106−5110.
(12) Shen, Y.; Johnson, M. A.; Martin, D. C. *Macromolecules* **1998**, *31*, 8857−8864.
(13) Lazo, N. D.; Downing, D. T. *Macromolecules* **1999**, *32*, 4700−4705.
(14) He, S. J.; Valluzzi, R.; Gido, S. P. *Int. J. Biol. Macromol.* **1999**, *24*, 187−195.
(15) Inoue, S. I.; Magoshi, J.; Tanaka, T.; Magoshi, Y.; Becker, M. *J. Polym. Sci. Part B: Polym. Phys.* **2000**, *38*, 1436−1439.
(16) Ashida, J.; Ohgo, K.; Asakura, T. *J. Phys. Chem. B* **2002**, *106*, 9434−9439.
(17) Sirichaisit, J.; Brookes, V. L.; Young, R. J.; Vollrath, F. *Biomacromolecules* **2003**, *4*, 387−394.
(18) Yao, J. M.; Nakazawa, Y.; Asakura, T. *Biomacromolecules* **2004**, *5*, 680−688.
(19) Zong, X. H.; Zhou, P.; Shao, Z. Z.; Chen, S. M.; Chen, X.; Hu, B.-W.; Deng, F.; Yao, W. H. *Biochemistry* **2004**, *43*, 11 932−11 941.
(20) Asakura, T.; Sugino, R.; Yao, J.; Takashima, H.; Kishore, R. *Biochemistry* **2002**, *41*, 4415−4424.
(21) Shimura, K. *Experientia* **1983**, *39*, 441−473.
(22) Kikuchi, Y.; Mori, K.; Suzuki, S.; Yamaguchi, K.; Mizuno, S. *Gene* **1992**, *110*, 151−158.
(23) Kaplan, D.; Wade, W. W.; Farmer, B.; Viney, C. In *Silk Polymers*; Kaplan, D., Wade, W. W., Farmer, B., Viney, C., Eds.; American Chemical Society: Washington, DC, 1994; Vol. 544, pp 2−16.
(24) Zhou, C. Z.; Confalonieri, F.; Medina, N.; Zivanovic, Y.; Esnault, C.; Yang, T.; Jacquet, M.; Janin, J.; Duguet, M.; Perasso, R.; Li, Z. G. *Nucl. Acids Res.* **2000**, *28*, 2413−2419.
(25) Mori, H.; Tsukada, M. *Rev. Mol. Biotechnol.* **2000**, *74*, 95−103.
(26) Nagarsekar, A.; Crissman, J.; Crissman, M.; Ferrari, F.; Cappello, J.; Ghandehari, H. *J. Biomed. Mater. Res.* **2002**, *62*, 195−203.
(27) Freddi, G. In *Polymeric Materials Encyclopedia*; Salamone, J. C., Ed.; CRC Press: New York, 1996; Vol. 1, pp 7734−7744.
(28) Tsukada, M. *J. Appl. Polym. Sci.* **1988**, *35*, 965−972.
(29) Tsukada, M.; Freddi, G.; Kasai, N.; Monti, P. *J. Polym. Sci. Part B: Polym. Phys.* **1998**, *36*, 2717−2724.
(30) Rathore, O.; Sogah, D. Y. *Macromolecules* **2001**, *34*, 1477−1486.
(31) Osanai, M.; Okudaira, M. *Amino Acids* **2001**, *20*, 113−121.
(32) Maji, T. K.; Basu, D.; Datta, C.; Banerjee, A. *J. Appl. Polym. Sci.* **2002**, *84*, 969−974.
(33) Yao, J. R.; Xiao, D. H.; Chen, X.; Zhou, P.; Yu, T. Y.; Shao, Z. Z. *Macromolecules* **2003**, *36*, 7508−7512.
(34) Anderson, J. P.; Cappello, J.; Martin, D. C. *Biopolymers* **1994**, *34*, 1049−1058.
(35) Zhou, P.; Xie, X.; Knight, D. P.; Zong, X.-H.; Deng, F.; Yao, W.-H. *Biochemistry* **2004**, *43*, 11 302−11 311.
(36) Chen, X.; Knight, D. P.; Shao, Z. Z.; Vollrath, F. *Polymer* **2001**, *42*, 9969−9974.
(37) Noda, I. *Appl. Spectrosc.* **1993**, *47*, 1329−1336.
(38) Nakano, T.; Shimada, S.; Saitoh, R.; Noda, I. *Appl. Spectrosc.* **1993**, *47*, 1337−1342.
(39) Czarnecki, M. A.; Maeda, H.; Ozaki, Y.; Suzuki, M.; Iwahashi, M. *Appl. Spectrosc.* **1998**, *52*, 994−1000.
(40) Smeller, L.; Heremans, K. *Vibr. Spectrosc.* **1999**, *19*, 375−378.
(41) Magtoto, N. P.; Sefara, N. L.; Richardson, H. H. *Appl. Spectrosc.* **1999**, *53*, 178−183.
(42) Noda, I.; Dowrey, A. E.; Marcott, C.; Story, G. M.; Ozaki, Y. *Appl. Spectrosc.* **2000**, *54*, 236A−248A.
(43) Eads, C. D.; Noda, I. *J. Am. Chem. Soc.* **2002**, *124*, 1111−1118.
(44) Hu, B.-W.; Zhou, P.; Noda, I.; Zhao, G.-Z. *Anal. Chem.* **2005**, *77*, 7534−7538.
(45) Zhou, P.; Li, G. Y.; Shao, Z. Z.; Pan, X. Y.; Yu, T. Y. *J. Phys. Chem. B* **2001**, *105*, 12469−12476.
(46) Monti, P.; Freddi, G.; Bertoluzza, A.; Kasai, N.; Tsukada, M. *J. Raman Spectrosc.* **1998**, *29*, 297−304.
(47) Monti, P.; Taddei, P.; Freddi, G.; Asakura, T.; Tsukada, M. *J. Raman Spectrosc.* **2001**, *32*, 103−107.
(48) The existence of a true cross-peak (1655, 1642) in the asynchronous spectrum is verified by the detailed examination of the numerical values of the spectrum.
(49) Li, G. Y.; Zhou, P.; Shao, Z. Z.; Xie, X.; Chen, X.; Wang, H. H.; Chunyu, L. J.; Yu, T. Y. *Eur. J. Biochem.* **2001**, *268*, 6600−6606.